Synthesis and Characterization of Alginate-Chitosan Nanocarrier System for Empagliflozin Delivery

Ramazanzadeh, Nasim; Mahmoodi, Nosrat Ollah*[+]

Faculty of Sciences, Department of Organic Chemistry, University of Guilan, Rasht, I.R. IRAN

ABSTRACT: *A biocompatible nanocarrier system was prepared by reacting Calcium Alginate (CA) with Chitosan (CS). The structure of synthesized nanocarrier chitosan-calcium alginate (CS-CA) was characterized using Thermo Gravimetric Analysis (TGA), Fourier Transforms InfraRed (FT-IR), Field Emission Scanning Electron Microscopy (FE-SEM), X-Ray Diffraction (XRD) Atomic Force Microscopy (AFM), and Transmission Electron Microscopy (TEM). Swellings of CS-CA and CA, and their ability for loading and in vitro release behavior of empagliflozin (EMP) were investigated. The results show that the capacity of loading on CS-CA is more than that of CA. For both nanocarriers, the release of the drug is higher in neutral pH (7.4 and 6.8) than in acidic pH (1.2). Although more release was observed for CA than CS-CA, the latter shows a favorable delay in the drug release in all pHs. As a result, CS-CA nanocarrier is suggested as a new candidate for an EMP colon drug delivery.*

KEYWORDS: *Nanocarrier; Chitosan-calcium alginate; Empagliflozin; Drug delivery systems.*

INTRODUCTION

The main challenges in the commercialization of drugs are the improvement of solubility, permeability, bioavailability, etc. In these regards, drug delivery systems provide a promising approach for researchers [1, 2]. Recently, with the advent of nanotechnology, a new class of nanocarriers has been designed that show several advantages including drug solubility improvement, reduced dose**,** sustained drug release, targeted drug delivery, bioavailability, etc [3, 4]. Synthetic [3, 5], the natural polymer [6, 7], and their combinations [8] used for drug delivery include a wide range of gums, mucilages, and polysaccharides. Natural polymers are non-toxic, biocompatible, inexpensive, and widely available. Among the polysaccharides, Sodium Alginate (SA) and Chitosan (CS) were used extensively for different drug delivery including anti-diabetic drugs [9-11]. SA is one of the natural polymers which are biodegradable and biocompatible provide coagulation in various drugs. SA is composed of (1-4)-linked-D-mannuronic acid (M) and -L-guluronic acid (G) in various arrangements and ratios. This biopolymer prepares hydrogels in the attendance of divalent cations e.g. Ca^{2+}, Ba^{2+}, Sr^{2+}, and Zn^{2+} which causes the drug to be enclosed in the matrix that allows for designing DDS [12,13]. Several investigators focused their consideration on the development of Calcium Alginate (CA) beads as controlled DDS for oral drugs [14-16]. CS is a linear, biological, and non-toxic polysaccharide compounded of D-glucosamine and *N*-acetyl-D-glucosamine units connected by β-(1-4) glycosidic linkages that are isolated by partial destruction of chitin and extensively applied for DDS [17-19]. Cross-linking of CA and CS in a bead is adapted to furnish useful biopolymer for medical and pharmaceutical investigation; the caught

** To whom correspondence should be addressed.*
+ E-mail: mahmoodi@guilan.ac.ir & nosmahmoodi@gmail.com
1021-9986/2021/4/1107-1118 12/$/6.02

systems are determined by increased stability in comparison to those obtained with single-polymer [20]. DDS of CA and CS nanocarrier has obtained great attention in recent years. For example, Nalini et al showed that the synthesized SA/CS NPs can be acted as the DDS such as quercetin to improve the therapeutic effects of the drug operation [21]. Empagliflozin (EMP) is an anti-diabetic drug with the (4-chloro-3- (4-[(3S)-tetrahydrofuran-3-yloxy]benzyl))phenyl chemical formula. EMP, appears to reduce the likelihood of hospitalization for heart failure or progression of chronic kidney disease in persons with type 2 diabetes. EMP may reduce the likelihood of death due to cardiovascular causes in people with type 2 diabetes who have known cardiovascular disease [22]. Therefore, the main aim of this work was the loading of this drug on a nanocarrier prepared by a combination of CS and CA in the framework of DDS to improve the medicinal effect of EMP.

EXPERIMENTAL SECTION

Materials

CS (MW: 50,000–190,000 kDa, deacetylation degree 85%), SA, acetic acid (AcOH) (99.7%), and were gotten from Sigma Aldrich Company. $CaCl_2$ anhydrate, Phosphate-Buffered Saline (PBS), HCl, NaOH, and EMP were all obtained from Merck Company.

Preparation of CA Beads.

CA beads were prepared by gelation method *via* Ca^{+2} as a cross-linking agent. Firstly, 0.1 g SA powder was dissolved into 20 mL purified water and stirred at Room Temperature (RT) for 6h. This solution was reserved for 24 h in a refrigerator, and then was dropped in 40 mL 1.25% solution of $CaCl_2$ below steady mild stirring, at RT. After 1 hour, the beads were composed, washed with deionized water, and dried at 50 °C overnight [23].

Preparation of Chitosan-calcium alginate (CS–CA) Beads.

SA solution (0.1%, w/v) was made by dissolving SA powder in water under magnetic stirring at RT. The solution of CS and $CaCl_2$ was ready by dissolving 0.04 g of CS and 0.5 g of $CaCl_2$ in 40 mL of 1% (v/v) AcOH; then, the SA solution was added drop by drop to CS and $CaCl_2$ solution for 60 minutes, and stirred in RT for 24h. The obtained beads CS-CA were filtered, rinsed with distilled water several times, and dried at 50 °C overnight in an oven.

Preparation of EMP Loaded CA-CS beads

For loading of EMP on premade nanocomposite, 0.1 g SA powder was dissolved into 20 mL of EMP solution with 250 ppm concentration and stirred in RT for 3h, the pH of the solution was adjusted to 7.0 using 0.1M NaOH. Then, 0.04 g CS and 0.5 g $CaCl_2$ were dissolved in 40 mL of AcOH 2% (v/v), pH of the solution was adjusted to 5.5 using 0.1M HCl and stirred for 24 h. Afterward, the solution of SA and EMP was added dropwise to CS and $CaCl_2$ solution for 80 min, the reaction mixture was continuously stirred for 3 h at RT. Nanocarriers were precipitated on the bottom of the reaction vassal. Nanocarriers were left in solution and washed with water to remove unreacted chemicals and then dried in an oven at 50 °C overnight.

Characterization

The FTIR spectrophotometer (8400S, Shimadzu) was applied to seek structural information in the limited area 4000-400 cm^{-1}. The surface morphology was inspected by a scanning electron microscope (SEM) (Hitachi S4160 model) fitted with an energy dispersive X-ray analyzer (EDAX). Thermogravimetric analysis of nanocarriers was investigated using the LENSES STAPT-1000 calorimeter (Germany) by scanning up to 700 °C with a heating rate of 10 °C/min. X-ray diffraction (XRD, Shibuya-ku, Japan) was recorded at RT on a RigakuD/Max-2550 powder diffractometer with a scanning rate of 5°/min, in the 2θ range of 10–70. An Atomic Force Microscope (AFM, model: Nano Wizard®II NanoScience AFM, JPK Instruments Inc., Germany) was applied to investigate the morphology of nanocarriers. Transmission electron microscopy analyses were performed using the TEM microscope (Philips CM120).

Swelling study

The swelling specifications of CA and CS-CA beads were defined by plunging dried test samples to swell in 5mL of a solution at pH 1.2 in 37°C for 2 h and then added into a pH 6.8 and 7.4 medium, simulating gastrointestinal tract conditions. At particular time intervals, samples were removed from the swelling medium and were blotted with a piece of paper towel to absorb excess water on the surface. The swelling ratios (Qs) of test samples were calculated from the following expression[24] :

$$Qs = (Ws - Wd)/Wd \quad (1)$$

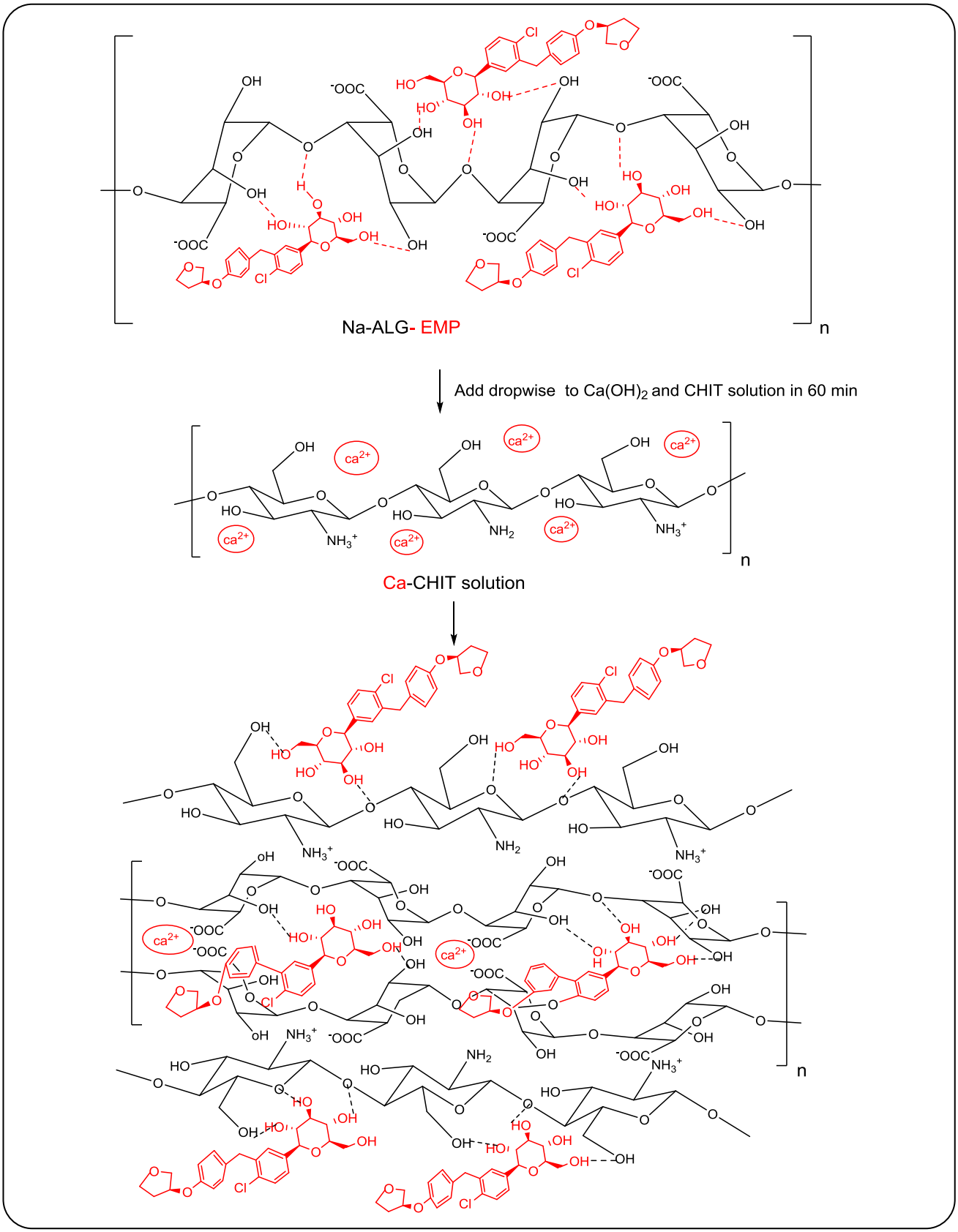

Fig. 1: Proposed prearrangement of EMP-loaded CA-CS nanocarrier beads.

Where *Ws* is the weight of the swollen test sample and Wd is the weight of the dried test sample. All experiments were conducted in triplicate.

MP loading efficiency

To calculate the EMP Loading Efficiency (LE), nanocarriers were filtered from the reaction mixture. The clear supernatant was analyzed for EMP content using PG Instruments T80UV-Visible spectrophotometer at 375.5 nm and the following equations[25].

LE (%) = [(Total amount of EMP-the free amount of EMP in the supernatant) / Total amount of EMP] ×100 (2)

EMP release studies

To study the release behavior of EMP from nanocarriers, the release process was investigated at 37◦C via a dialysis bag with 5000 Da molecular cut-off at three different pHs. The loaded nanocarrier (80 mg) was suspended in a Phosphate Buffer Saline solution (PBS) (5 mL, pH 1.2, 6.8, and 7.4). Then it was poured into the dialysis bag and was incubated in PBS buffer (50 mL) of the same pH value at 37°C under shaking (200 rpm). A certain value (3 mL) of solution from the container was removed after every time step, making sure to replace it with the same amount of fresh PBS solution. The amount of the released EMP was measured at different time points from 0 h to 12 h by a UV-Vis spectrophotometer (375.5 nm) [26].

Release (%) = [Release EMP / Total amount of EMP] × 100 (3)

RESULTS AND DISCUSSION

Characterization of the Carbo-bio Nanocarrier

Fig. 2 represents the FT-IR spectra of CS (a), SA (b), CS-CA (c), EMP (d) and CS-CA-EMP (e). CS showed a broad peak at 3400 cm^{-1} that belonged to N–H and O–H stretching of CS molecules. The peak at 2800-2950 cm^{-1} is attributed to the –C-H stretching. The peaks at 1648 and 1741cm^{-1} correspond to NH and C=O amide bending vibrations respectively, as well as peaks at 1156, 1091, and 1033 cm^{-1} associated with asymmetric vibrations of C-O-C. In the FT-IR spectrum of SA, broad peaks at 3400, 1416, 1617, and 1297 cm^{-1} are assigned to O–H stretching, an asymmetric symmetric and symmetric stretching of the –COO, and stretching of

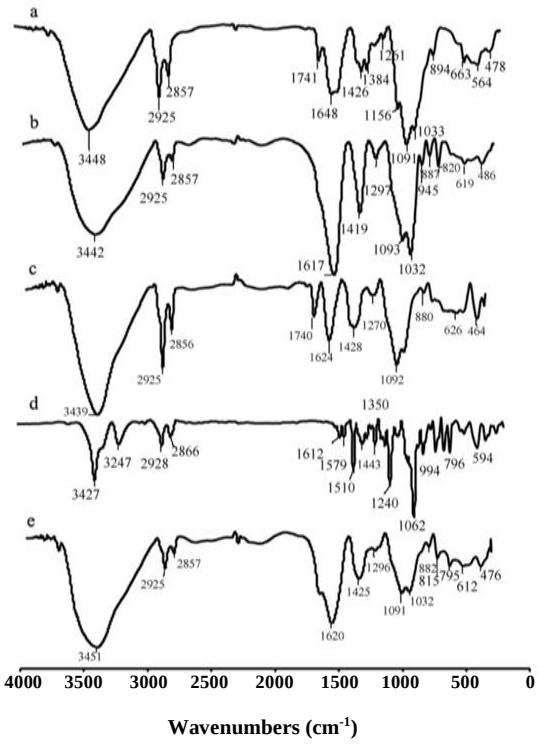

Fig. 2: Profiles of FT-IR spectrum CS (a), SA (b), CS-CA (c), EMP (d) CS-CA-EMP (e).

C-O groups [27]. In the FT-IR spectrum of nanocarrier CS-CA (c) characteristic symmetric stretching –COO was shifted from1617 to 1624 cm^{-1}. This change reflects the creation of an ionic bond between calcium ions and carboxylic ions and also the peaks were slightly expanded in the regions of 1400 and 900-1100 cm^{-1}. These changes showed the relations between SA, $Ca^{+2,}$ and CS. The spectra of EMP (d), The bands at 3400, 3000, and 2800-2900 cm^{-1} are related to the OH, =CH of the aromatic ring and $–CH_2$ groups respectively. Due to the presence of aromatic rings and ether groups in the structure of EMP, the corresponding peaks appeared in the regions between 1400- 1600 cm^{-1} and 1000-1200 cm^{-1}. Finally, the spectrum of nanocarrier that is loaded with the drug (e), shows all the expected vibration bands of its constituents, confirming their contribution to the final nanocarrier Also, in this spectrum, the peaks in the region of 3000-3400., 1600-1700, 1400-1500, and 1000-1100 cm^{-1} were expanded that is probably related to the electrostatic interactions and the formation of hydrogen bonds between functional groups on the nanocarrier and drug.

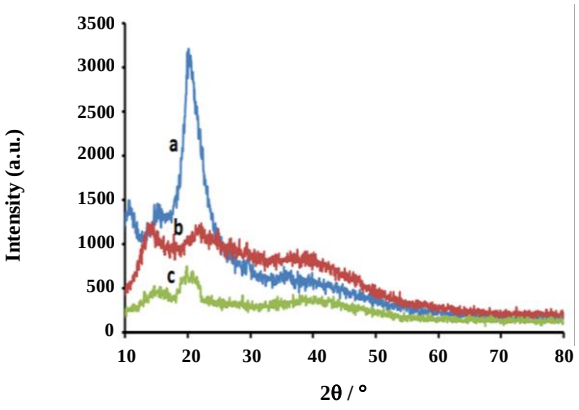

Fig. 3: X-ray diffractogram of CS (a), SA (b) and CS-CA (c).

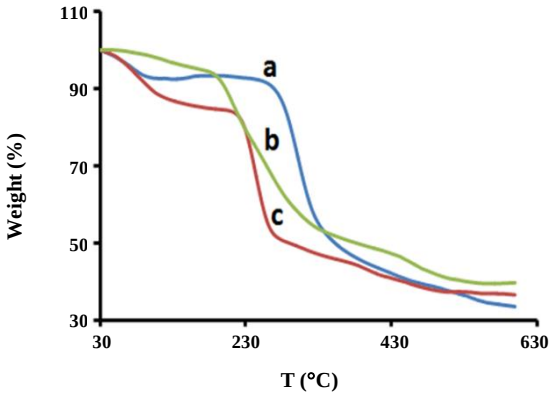

Fig. 4: Thermogravimetric analysis (TGA) of CS (a), SA (b), and CS-CA (c).

XRD patterns

The crystallographic structure of the nanocarrier was determined by XRD technique. Fig. 3 shows the XRD patterns of the CS (a), SA (b), and CS-CA (c). In Fig.3 (a), the typical peak of CS is observed at 2θ = 20–22°, representing the amorphous structure of CS. The X-ray diffraction pattern of SA Fig.3 (b) is considered by the presence of two peaks at 2θ = 13° and 22°, according to the literature data. Finally, Fig.3 (c) shows the XRD patterns of the nanocarrier, in addition, to peaks of SA and CS at 2θ = 13-15°and 19-22°, one expanded peak was observed at 2θ = 40° which probably corresponds to the presence of calcium ions in the nanocarrier [28-30].

Thermal study

Thermal analysis has been widely used for the characterization of polymeric materials. The Thermo Gravimetric Analysis (TGA) of CS (a), SA (b), and CS-CA (c) is presented in Fig.4. During the first stage below 150◦C of CS degradation (Fig. 4a), a slight loss of mass was observed that attributed to water evaporation. The second stage, with a significant loss of mass between 250-350◦C, was due to the decomposition of the CS backbone. The primary weight loss for SA (b) below 130°C was due to the evaporation of the adsorbed water, and the maximum weight loss temperature occurred around 220-250°C, which corresponded to the decomposition of its organic structure of it. In the below curve of nanocarrier (c), a first mass loss at below 150°C was attributed to volatile desorption, mainly moisture. The second loss started from 200°C until 330°C with low slope than (a) and (b) curve that related to the decomposition of nanocarrier that contains SA, CS, and calcium ions with electrostatic interactions and the formation of hydrogen bonds between them [22, 31, 32].

FE-SEM AND EDX analyses

The surface morphology of the CS (a), SA (b), CS-CA (c), and noncarrier with the drug (d) was confirmed using FE-SEM (Fig. 5). These images show that CS and SA have smooth surfaces with some holes (a and b). These images show the smooth surface of CS and SA with some holes.

As can be seen from the image of the nanocarrier (3c), after preparation of the nanocarrier with the addition of calcium and CS solution to SA solution, some spherical beads tightly joined together and formed aggregates. This morphology probably corresponds to the interaction between the components of the nanocarrier. Different morphology of nanocarrier with the drug has been shown in (3d). The EDAX spectra confirmed the presence of relevant elements on the surface of the nanocarrier (e,f).

After the preparation of the nanocarrier with the addition of calcium and CS solution to SA solution, as it can be seen from the image of nanocarrier (c), it is obvious that some spherical beads that tightly joined together and form aggregates. This morphology probably corresponds to the interaction between the content materials of the nanocarrier. Following, different morphology of nanocarrier with the drug has been shown in the image (d). Also, from the EDAX spectra in Fig. 5 (e) and (f) the presence of elements on the nanocarrier is clear.

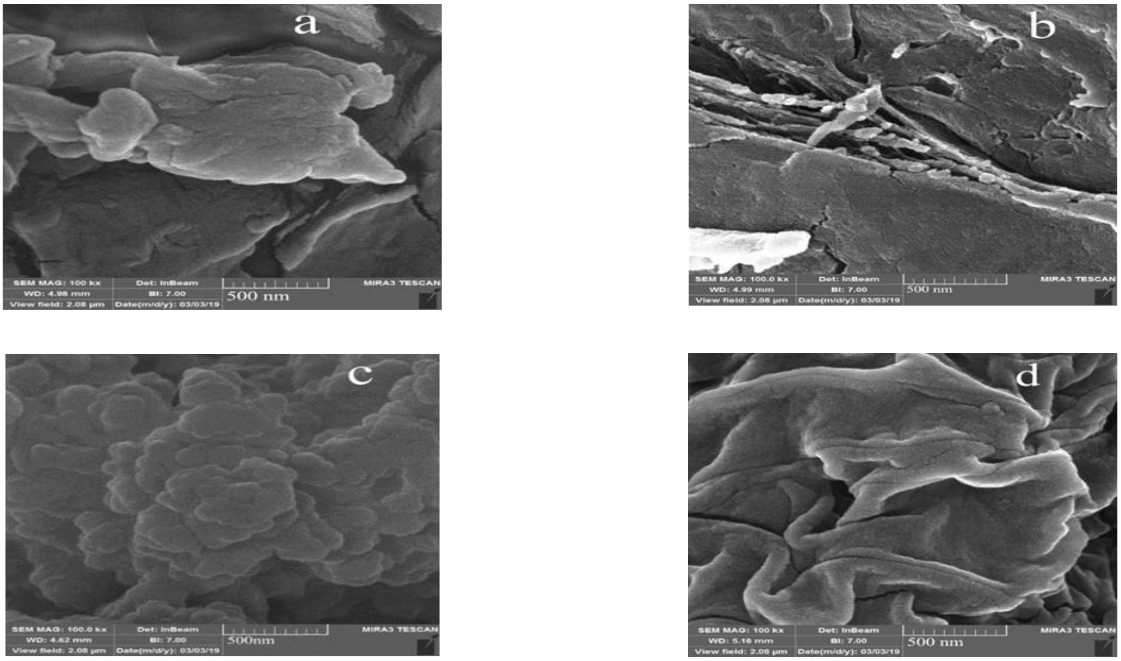

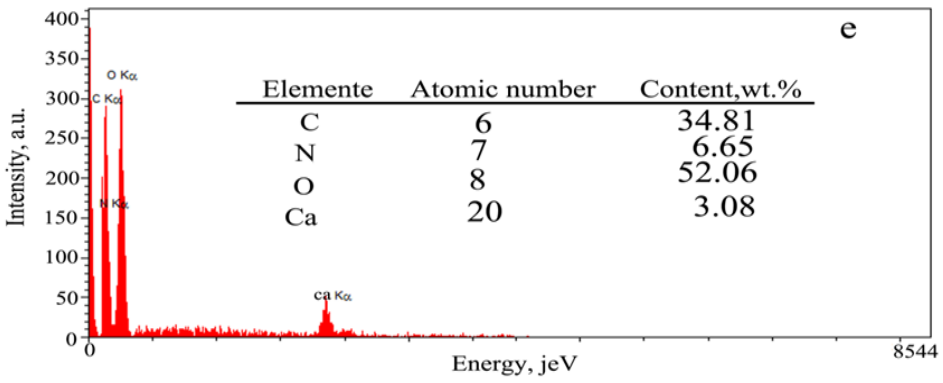

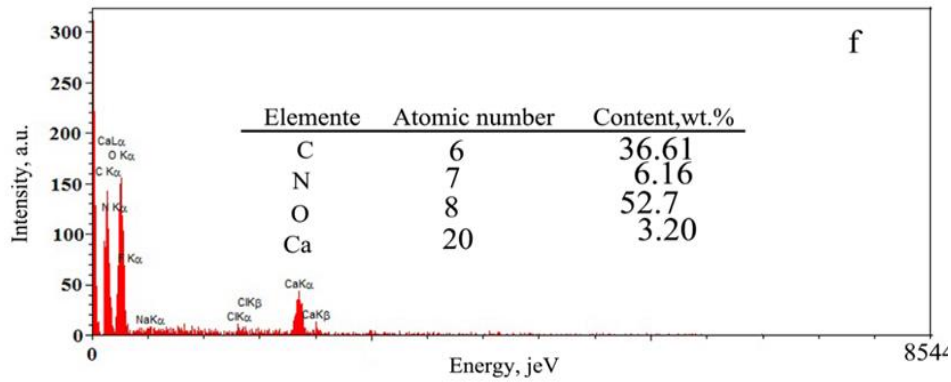

Fig. 5: FE-SEM analysis of CS (a), SA (b) and CS-CA (c), CS-CA- EMP (d) and EDAX, CS-CA (e) CS-CA- EMP (f).

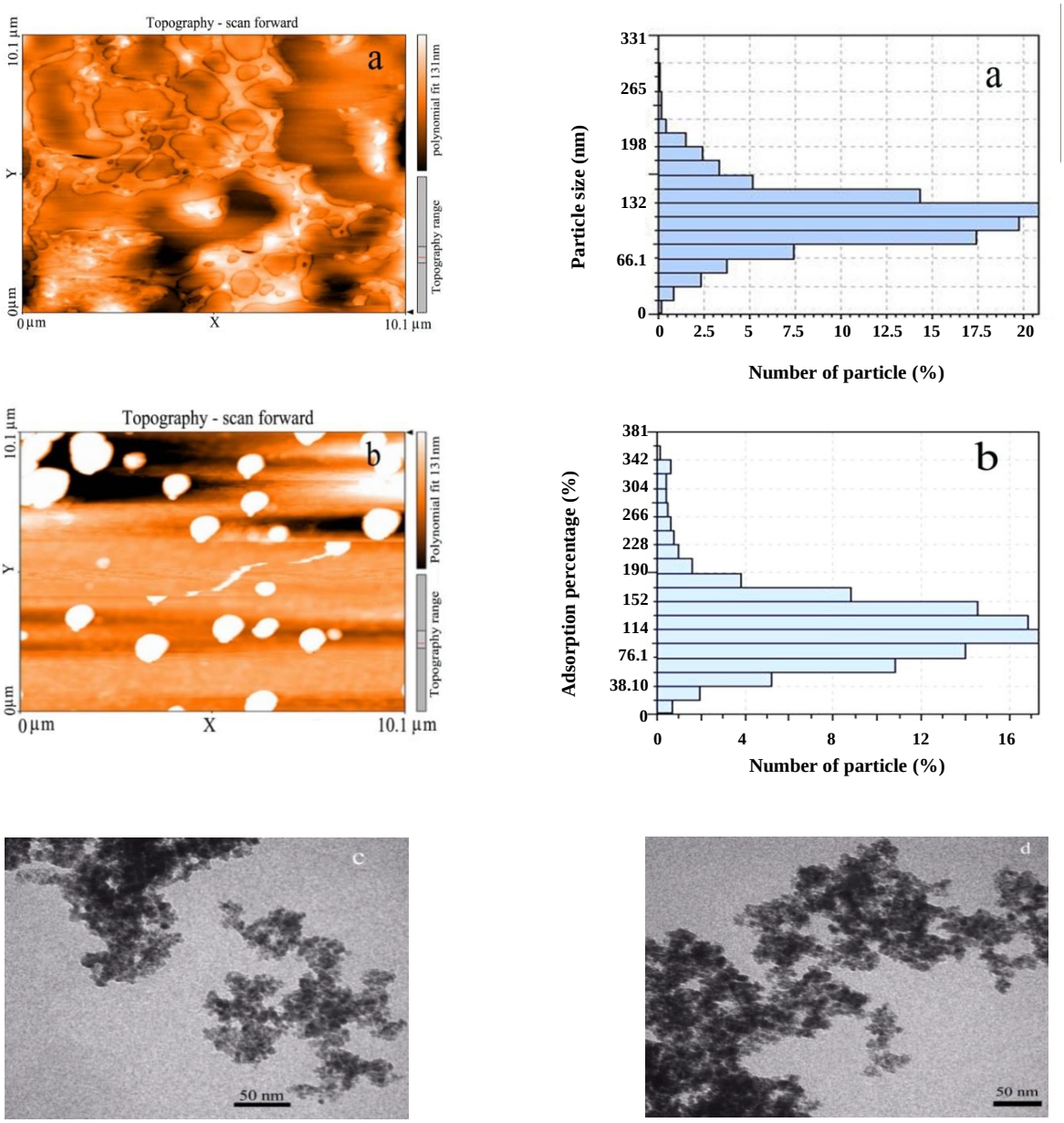

Fig. 6: AFM(a,b(drug)) and TEM(c,d(drug)) image of CS-CA and CS-CA -Drug.

TEM and AFM analysis

Based on the AFM and TEM images in Figs.6 (a,b) and (c,d), the size of particles varied within 50-95 nm; moreover, the drug loading had no significant effect on the morphology of nanoparticles.

Swelling studies

Some natural polymers like SA, CA, and CA-CS polymers have good potential for the swelling process when in contact with fluid with different pH. This property is owing to the presence of hydrophilic groups in their structure. With adsorption, the fluid is water, the polymer chain is swollen without destruction. This factor is very important in drug delivery, therefore, the swelling property of CA and of CA-CS was investigated in phosphate buffer solutions with three pH (1.2, 6.8, and 7.4) that simulated gastric and intestinal fluid. Fig. 6, 7, and 8 show their swelling behavior of them.

At pH 1.2 (Fig 6), there are no variances in the swelling ability of the CA and CS-CA at this condition, the ester

groups of the SA protonated to alginic acid. The insolubility of this compound in these conditions and its ability to form hydrogen bonding, inhibit the swelling of these nanocarrier beads. Similar swelling behavior is observed for CS-CA. In an acidic condition, CS is very soluble and its amine units are converted into soluble NH^{4+} ions. However, the interaction of amino groups and ester groups is not strong enough to stimulate swelling. Thus, the restricted total swelling behavior is ruled by the CA structure. Figs 7 and 8, show the swelling ability of CA and CS-CA at pH (6.8 and 7.4). As can be seen in both figures, increasing contact time from 5 to 60 minutes leads to increased swelling of the systems and then remains approximately constant. This performance can be attributable to ion exchange reaction amongst Na^{+} (in the phosphate buffer) and Ca^{2+} coordinated to COO groups of SA. This displacement of ions leads to a variation in the structure by creating a gap between the carbohydrate chain, which causes the penetration of the liquid and the swelling of the system. This process continues pending the osmotic pressure into the beads equilibriums the strength of the cross-linking bonds and physical entanglements, electrostatic attractive forces, and hydrogen bonding, that arrangement the structure of the beads. As a result, nanocarrier starts to decompose, and their weight decreases. The results obtained from the swelling study evidence that CS-CA beads are more resistant structures compared to CA, this feature may be related to the interactions among CS and SA chains. The maximum swelling degree of CS-CA systems is able to reach a swelling balance in about 40 minutes and to keep their weight at a constant level till the end of the test. Possibly the interactions among the two polymers are accountable for the formation of nanocarrier particles with significant mechanical resistance, which limits the liquid uptake and the structure breakdown. These results are in good agreement with other studies on different cases. Similarly, the increase in pH leads to an increase in swelling [32-34].

EMP loading efficiency and pH effects

The most important concerns in the novel DDS are the loading of the drug on nanocarriers. In this regard, the pH factor is an essential element affecting the efficient loading of the drug from aqueous solutions. The dependence of drug adsorption on the pH factor is closely connected with the type of functional groups existing in the carrier's

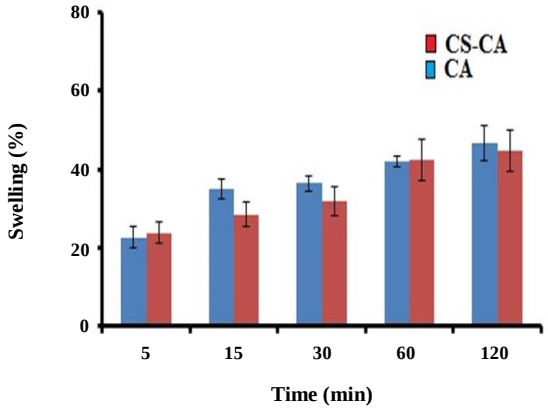

Fig. 7: Swelling characteristics of CS-CA and CA in a solution at pH 1.2 for 2 h and at 37°C ±1.

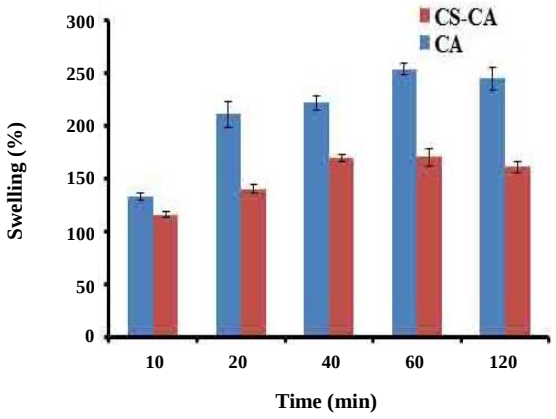

Fig. 8: Swelling characteristics of CS-CA and CA in a solution at pH 6.8 for 2 h and at 37°C ±1.

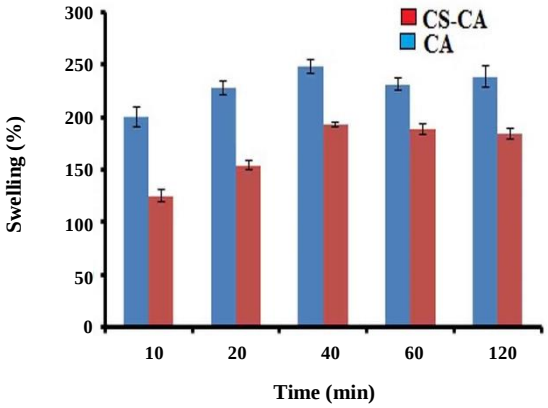

Fig. 9: Swelling characteristics CS-CA and CA in a solution at pH 7.4 for 2 h and at 37°C ±1.

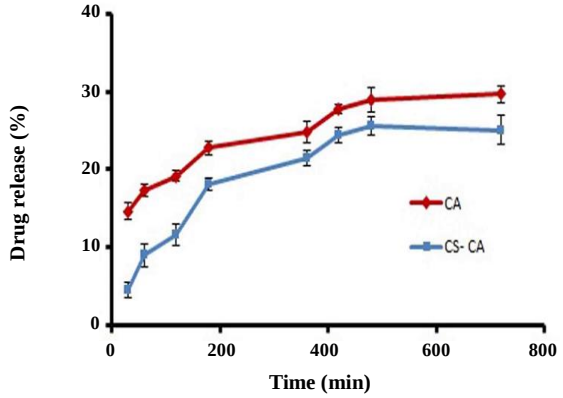

Fig. 10: Curves of EMP release from CA and CS-CA in an acidic environment with pH 1.2.

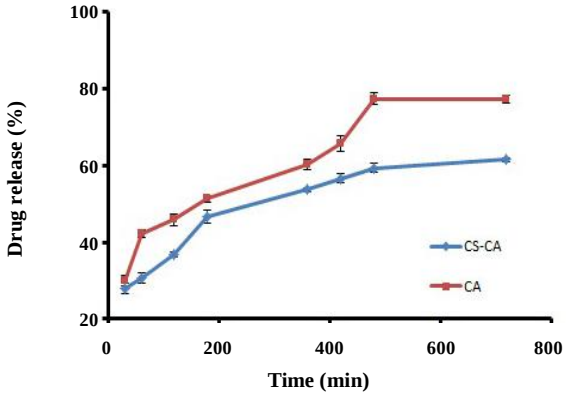

Fig. 11: Curves of EMP release from CA and CS-CA in phosphate buffer at pH 6.8.

surface as well as drug solution chemistry. Therefore, in this work, EMP loading on CA and CS-CA nanocarriers was studied in different pH values 3-9. The optimal pH was found to be 6.2 where the loading efficiency measured using the UV-Vis spectrophotometer was about 58.48 and 81.65% for CA and CS-CA, respectively. This observation was related to the surface of the nanocarrier under pH 4, CS is mainly protonated, while SA, as well as drug, is unionized. Therefore, drug and surface make weak interactions leading to low drug loading. Whereas, with an increase in pH (above 4) -COOH on SA (pKa ~3.4-4.4) is deprotonated to $-COO^-$ which could form complex with CS and make a stable structure that could probably interact with the drug through hydrogen bonding and electrostatic interaction that results in the increasing percentage of drug loading. In the higher pH, CS is deprotonated which causes the partial destruction of polyelectrolyte complexes resulting in decreased EMP loading.

In vitro release study

The EMP release percentage obtained from loaded CA and CS-CA at a pH of 1.2, 6.8, and 7.4 indicated (Fig. 9-11). In the acidic medium % EMP released during two hours is quite low and varies between 11.59% and 19.16% (Fig.9). The delay (postponement) of release can be attributed to the reduced swelling ability of nanocarrier in this circumstance. These results indicate that to minimize EMP delivery in an acidic condition it is better to promote and favor this procedure at the intestinal level. [35,36]

Fig.10, shows the EMP release activities in phosphate buffer at pH 6.8. In this condition, the systems primarily swell and then started to erode and disintegrate, as a result, CA is able to release 77% of EMP during ~ 8 hours; by contrast, the amount of drug released from CS-CA particles is 59% during the same period. This difference corresponds to the stronger electrostatic interaction and hydrogen bonding between functional groups on the CA, CS, and EMP to compare pure CA which improves the mechanical and fluid uptake resistance of the polymeric network at pH 6.8 [37].

Fig.11, shows the amount of drug release from CA and CS-CA particles at pH 7.4. As is clear, there are no significant differences between CA and CS-CA in the drug release compared to pH 6.8, but more quantities of the drug have been released in these conditions. So, these values were 94% and 77% for CA and CS-CA respectively. These increases in the release of drugs probably are related to the partial destruction of polyelectrolyte complexes between CS and CA. Such as pH 6.8, when CS is in the particles, the drug release rate decreases. In phosphate buffer solutions, CS-CA particles need longer times to deliver EMP compared to CA. Probably the presence of the CS-CA complex creates a crumpled and irregular structure which makes the drug release difficult [38,39].

CONCLUSIONS

Here, for the first time, the possibility of loading EMP as an antidiabetic drug on CA and CS-CA nanocarrier using an inotropic pre-gelation technique was investigated. The structure of the nanocarrier was assigned by FT-IR, XRD, TGA, and SEM. The maximum loading of the EMP on CS-CA (81.65%) was determined at pH 6.2. the swelling study of the carrier at three different pHs (1.2, 6.8, and 7.4) shows that the highest swelling occurred

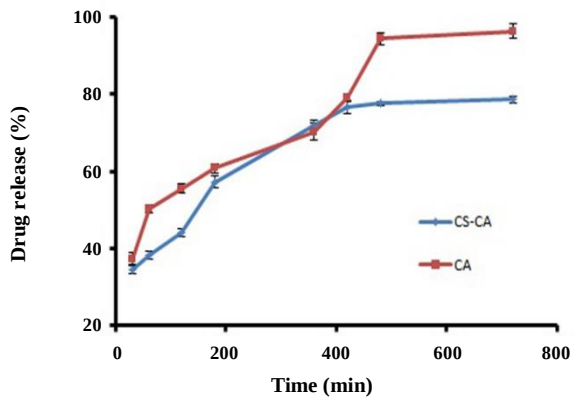

Fig. 12: Curves of EMP and CS-CA in phosphate buffer at pH 7.4.

at pH 7.4. The consequences of the EMP release study showed that part of it was released after contact with a carrier with gastric simulated fluid, but the EMP was broadly released at intestinal pH. The maximum release of EMP from CA and CS-CA at pH 7.4 after 8 hours was 94% and 77% respectively. The results suggested that the presence of CA in the structure of CS–CA nanocarriers were found to retard meaningfully the release from the beads and led to an increase in the strength of encapsulation efficiency. Therefore, CA and CS–CA could be suitable polymeric carriers for the controlled release of EMP.

Received : Mar. 12, 2022 ; Accepted : Jun. 10, 2022

REFERENCES

[1] Mahmoodi N.O., Alavi, S.M., Yahyazadeh, A., Formulation and Therapeutic Efficacy of PEG-Liposomes of Sorafenib for the Production of NL-PEG-SOR FUM and NL-PEG-SOR TOS. *Res. Chem. Intermed.*, **48**: 3915–3935 (2022).

[2] Zhu J., Zhong L., Chen W., Song Y., Qian Z., Cao X., Huang Q., Zhang B., Chen H., Chen W., Preparation and Characterization of Pectin/Chitosan Beads Containing Porous Starch Embedded with Doxorubicin Hydrochloride: A Novel and Simple Colon Targeted Drug Delivery System, *Food Hydrocolloids*, **95**:562-570 (2019).

[3] Englert C., Brendel J.C., Majdanski T.C., Yildirim T., Schubert S., Gottschaldt M., Windhab N., Schubert U.S., Pharma Polymers in the 21st Century: Synthetic Polymers in Drug Delivery Applications, *Prog. Polym. Sci.*, **87**:107-164 (2018).

[4] Peng C., Huang Y., Zheng J., Renal Clearable Nanocarriers: Overcoming the Physiological Barriers for Precise Drug Delivery and Clearance, *J. Controlled Release*, **10(322)**:64-80 (2020).

[5] Gadadare R., Mandpe L., Pokharkar V., Ultra Rapidly Dissolving Repaglinide Nanosized Crystals Prepared Via Bottom-Up and Top-Down Approach: Influence of Food on Pharmacokinetics Behavior, *AAPS PharmSciTech*, **16**: 787-799 (2015).

[6] Bassas-Galia M., Follonier S., Pusnik M., Zinn M., Natural Polymers: A Source of Inspiration, in: "Bioresorbable Polymers for Biomedical Applications", Elsevier, 31-64 (2017).

[7] Tong X., Pan W., Su T., Zhang M., Dong W., Qi X., Recent Advances in Natural Polymer-Based Drug Delivery Systems, *React. Funct. Polym.*, **148**: 104501 (2020).

[8] Prajapati S.K., Jain A., Jain A., Jain S., Biodegradable Polymers and Constructs: A Novel Approach in Drug Delivery, *Eur. Polym. J.*, **1(120)**: 109191 (2019).

[9] Kumar S., Bhanjana G., Verma R.K., Dhingra D., Dilbaghi N., Kim K.H., Metformin- Loaded Alginate Nanoparticles as an Effective Antidiabetic Agent for Controlled Drug Release, *J. Pharm. Pharmacol.*, **69**:143-15 (2017).

[10] Rani R., Dahiya S., Dhingra D., Dilbaghi N., Kim K.-H., Kumar S., Evaluation of Anti-Diabetic Activity of Glycyrrhizin-Loaded Nanoparticles in Nicotinamide-Streptozotocin-Induced Diabetic Rats, *European Journal of Pharmaceutical Sciences*, **106**: 220-230 (2017).

[11] Chauhan P., Mahajan S., Prasad G., Preparation and Characterization of CS-ZnO-NC Nanoparticles for Imparting Anti-Diabetic Activities in Experimental Diabetes, *Journal of Drug Delivery Science and Technology*, **52**: 738-747(2019).

[12] Amirmahani N., Mahmoodi N. O., Mohammadi Galangashd M., Ghavidasta A., Advances in Nanomicelles for Sustained Drug Delivery, *J. Ind. Eng. Chem.*, **55(25)**: 21-34 (2017).

[13] Soltani A., Erfani-Moghadam, V., Yahyazadeh A., Mahmoodi N.O., Synthesis, Spectroscopic Characterization, Molecular Docking, as Well as in Vitro Cytotoxicity of Calcium-Sulfasalazine Compl, *J. Mol. Struct.*, **1267(5)**: 133568 (2022).

[14] Chegeni M., Rozbahani Z.S., Ghasemian M., Mehri M., Synthesis and Application of the Calcium Alginate/SWCNT-Gl as a Bio-Nanocomposite for the Curcumin Delivery, *Int. J. Biol. Macromol.*, **1(156)**: 504-513 (2020).

[15] Nesamony J., Singh P.R., Nada S.E., Shah Z.A., Kolling W.M., Calcium Alginate Nanoparticles Synthesized Through a Novel Interfacial Cross-Linking Method as a Potential Protein Drug Delivery System, *J. Pharm. Sci.*, **101**: 2177-2184 (2012).

[16] Zhang R., Lei L., Song Q., Li X., Calcium Ion Cross-Linking Alginate/Dexamethasone Sodium Phosphate Hybrid Hydrogel for Extended Drug Release, Colloids Surf. B. *Biointerfaces*, **175**:569-575 (2019).

[17] Shafabakhsh R., Yousefi B., Asemi Z., Nikfar B., Mansournia M.A., Hallajzadeh J., Chitosan: A Compound for Drug Delivery System in Gastric Cancer-A Review, *Carbohydr. Polym.*, 116403 (2020).

[18] Nalinbenjapun S., Ovatlarnporn C., Chitosan-5-Aminosalicylic Acid Conjugates for Colon-Specific Drug Delivery: Methods of Preparation and in Vitro Evaluations, *Journal of Drug Delivery Science and Technology*, **57**: 101397(2019).

[19] Ren G., Clancy C., Tamer T.M., Schaller B., Walker G.M., Collins M.N., Cinnamyl O-amine Functionalized Chitosan as a New Excipient in Direct Compressed Tablets with Improved Drug Delivery, *Int. J. Biol. Macromol.*, **141**: 936-946 (2019).

[20] Berger J., Reist M., Mayer J.M., Felt O., Peppas N., Gurny R., Structure And Interactions in Covalently and Ionically Crosslinked Chitosan Hydrogels for Biomedical Applications, *European Journal of Pharmaceutics and Biopharmaceutics*, **57**:19-34 (2004).

[21] Nalini T., Basha S.K., Sadiq A.M.M., Kumari V.S., Kaviyarasu K., Development and Characterization of Alginate/Chitosan Nanoparticulate System for Hydrophobic Drug Encapsulation, *Journal of Drug Delivery Science and Technology*, **52**: 65-72 (2019).

[22] Zelniker T.A., Wiviott S.D., Raz I., Im K., Goodrich E.L., Bonaca M.P., Mosenzon O., Kato E.T, Cahn A., Furtado R.H., Bhatt D.L., Leiter L.A., McGuire D.K., Wilding J.P., Sabatine M.S., SGLT2 Inhibitors for Primary and Secondary Prevention of Cardiovascular and Renal Outcomes in Type 2 Diabetes: A Systematic Review and Meta-Analysis of Cardiovascular Outcome Trials, *Lancet*, **393(10166)**: 31–39 (2019)

[23] Peniche C., Howland I., Carrillo O., Zaldıvar C., Argüelles-Monal W., Formation and Stability of Shark Liver Oil Loaded Chitosan/Calcium Alginate Capsules, *Food Hydrocolloids*, **18**: 865-871(2004).

[24] Amir Mahani N, Mahmoodi N.O., Ghavidast A., A Comparative Study on the Nanoparticles for Improved Drug Delivery Systems, *J. Photochem. Photobiol. B, Biol.*, **152(12)**: 681-693 (2016).

[25] Das R.K., Kasoju N., Bora U., Encapsulation of Curcumin in Alginate-Chitosan-Pluronic Composite Nanoparticles for Delivery to Cancer Cells, Nanomedicine: Nanotechnology, *Biology and Medicine*, **6**:153-160 (2010).

[26] Nunthanid J., Puttipipatkhachorn S., Yamamoto K., Peck G.E., Physical Properties and Molecular Behavior of Chitosan Films, *Drug Dev. Ind. Pharm.*, **27**:143-157 (2001).

[27] Hua S., Ma H., Li X., Yang H., Wang A., pH-Sensitive Sodium Alginate/poly (vinyl alcohol) Hydrogel Beads Prepared by Combined Ca^{2+} Crosslinking and Freeze-Thawing Cycles for Controlled Release of Diclofenac Sodium, *Int. J. Biol. Macromol.*, **46**:517-523 (2010).

[28] Soulairol I., Sanchez N., -Ballester M., Aubert A., Tarlier N., Bataille B., Quignard F., Sharkawi T., Evaluation of the Super Disintegrant Functionnalities of Alginic Acid and Calcium Alginate for the Design of Orodispersible Mini Tablets, *Carbohydr. Polym.*, **197**:576-585(2018).

[29] Tripathi S., Mehrotra G., Dutta P., Physicochemical and Bioactivity of Cross-Linked Chitosan–PVA Film for Food Packaging Applications, *Int. J. Biol. Macromol.*, **45**:372-376 (2009).

[30] Wu T., Li Y., Shen N., Yuan C., Hu Y., Preparation and Characterization of Calcium Alginate-Chitosan Complexes Loaded with Lysozyme, *J. Food Eng.*, **233**: 09-116 (2018).

[32] Mahmoodi N.O., Parvizi J., Sharifzadeh B., Rassa M., Facile Regioselective Synthesis of Novel Bis-Thiazole Derivatives and Their Antimicrobial Activity, *Arch. Pharm.*, **346**:860-864 (2013).

[33] Rineh A., Mahmoodi N., Abdollahi M., Foroumadi A., Sorkhi M., Shafiee A., Synthesis, Analgesic and Anti- Inflammatory Activity of 4- (2-phenoxyphenyl) Semicarbazones, Archiv Der Pharmazie, *An International Journal Pharmaceutical and Medicinal Chemistry*, **340**:409-415 (2007).

[34] Mollayousefi Samadi H., Fallah Shojaei A., Mahmoodi N.O., Preparation, Characterization, and Performance Study of PVDF Nanocomposite Contained Hybrid Nanostructure TiO_2-POM Used as a Photocatalytic Membrane, *Iran. J. Chem. Chem. Eng. (IJCCE)*, **40(1)**: 35-47 (2021).

[35] Chen S.-C., Wu Y.-C., Mi F.-L., Lin Y.-H., Yu L.-C., Sung H.-W., A Novel pH-Sensitive Hydrogel Composed of N, O-Carboxymethyl Chitosan and Alginate Cross-Linked By Genipin for Protein Drug Delivery, *J. Controlled Release*, **96**:285-300 (2004).

[36] Basu S.K., Rajendran A., Studies in the Development of Nateglinide Loaded Calcium Alginate and Chitosan Coated Calcium Alginate Beads, *Chem. Pharm. Bull.*, **56**:1077-1084 (2008).

[37] Irfan A., Imran M., Waseem Mumtaz A., Asim Raza Basra M., Molecular Docking and Computational Exploration of Isolated Drugs from Daphne Species Against COVID-19, *Iran. J. Chem. Chem. Eng. (IJCCE)*, **40(6)**: 2019-2027 (2021).

[38] Demirtaş G., Dege N., Ağar E., Şahin S., The Crystallographic, Spectroscopic and Theoretical Studies on (E)-2-[((4-Fluorophenyl)Imino)Methyl]-4-Nitrophenol and (E)-2-[((3-Fluorophenyl)Imino) Methyl]-4-Nitrophenol Compounds, *Iran. J. Chem. Chem. Eng. (IJCCE)*, **37(5)**:55-65 (2018).

[39] Belletire J.L., Mahmoodi N.O., γ-Butyrolactone Natural Products via Tributyltin-Hydride-Mediated Radical Cyclizations, *Journal of Natural Products*, **55(2)**:194-206 (1992).